[15]Daidzic, N., Stadler, R., and Dominick, J., "Experimental Techniques for Measurement of Droplet Evaporation," *Proceedings of the 8th International Conference on Liquid Atomization and Spray Systems*, National Inst. of Standards and Technology, Rouen, France, 1994, pp. 875–882 (ICLASS-94).
[16]Thomson, W. T., *Theory of Vibration with Applications*, 2nd ed., Prentice–Hall, Englewood Cliffs, NJ, 1981.
[17]Lide, D. R., *Handbook of Chemistry and Physics*, 70th ed., CRC Press, Boca Raton, FL, 1990.

Small Cavitating Venturi Performance Characteristics at Low Inlet Subcooling

I. Y. Chen,* S. G. Liou,* and J. S. Sheu†
National Yunlin University of Science and Technology, Yunlin 640, Taiwan, Republic of China

Introduction

CAVITATING venturis (CVs) are used to provide a passive flow control in many liquid flow systems. When liquid flow cavitates at the throat of a venturi, it can provide a choked flow regime useful for flow control. If the liquid's inlet pressure and temperature are fixed, a wide range of downstream pressures may be imposed with no effect on flow.[1] Under normal operation, the cavitating venturi is designed to provide cavitation at the throat so that the flow rate is independent of the downstream pressure. With cavitation, the flow at the throat is choked and the throat pressure (P_{th}) is equal to the saturation pressure at the inlet temperature [$P_{sat}(T_{in})$]. In typical applications, the CV inlet subcooling, dP_{sub}, which is defined as the pressure difference between the inlet pressure (P_{in}) and $P_{sat}(T_{in})$, is typically in the order of 700–1400 kPa.

There was a special application for CVs in the two-phase ammonia active thermal control system on the U.S. Space Station Freedom (SSF) in 1990. Here, the CVs were intended to be operated under conditions that were quite different from the typical applications. These CVs had very low inlet subcooling (40–140 kPa) and very small throat diameters. Prototypic CVs were included in the ground test article (GTA), a prototypic SSF active thermal control system (ATCS) two-phase thermal loop. During operation of the GTA in 1991, an anomalous CV overflow behavior was observed. Here the flow is a liquid nonchoked flow throughout the venturi and flows at a higher mass flow rate than the cavitation limit of the choked flow rate. Following the discovery of CV overflow, a series of experiments were performed to gain understanding of the CV's overflow phenomenon and to define its limits.[2]

The overflow phenomenon of the CVs found in the GTA ammonia testing was understood after the testing. The generic phenomenon of CV overflow and recovery from overflow in various liquids was not well understood. Overflow would still be a problem for a system of parallel CVs with low inlet subcooling. The objective of this study was to conduct a test on small cavitating venturis with water at low inlet subcooling to observe the phenomenon of overflow. The results were correlated to provide understanding of the overflow phenomenon.

Received Nov. 24, 1997; revision received April 20, 1998; accepted for publication April 22, 1998.

*Associate Professor, Department of Mechanical Engineering.
†Graduate Student, Department of Mechanical Engineering.

Flow Equations and Relative Parameters

Normal Operation

A typical cavitating venturi is shown in Fig. 1. During normal operation, cavitation occurs at the throat, and the throat pressure is $P_{sat}(T_{in})$. Therefore, the CV's choked mass flow rate (M_c) can be determined from the Bernoulli's equation (assuming that the frictional loss in the convergent section is negligible) as

$$M_c = A_{th}[2\rho(P_{in} - P_{sat}(T_{in})]^{0.5} \quad (1)$$

where A_{th} is the CV throat area and ρ is the liquid density. For a nonchoked condition, the pressure drop is driven by the loss coefficient, K_v. The flow through the CV is all liquid, and K_v can be defined as $K_v = 2(P_{in} - P_{out})/(\rho V_{th}^2)$, where $V_{th} = M_{liq}/(\rho A_{th})$ is the throat liquid velocity, and P_{out} is the outlet pressure. K_v must be applied to account for the nonchoked flow rate, M_{nc}, through the venturi

$$M_{nc} = A_{th}[2\rho(P_{in} - P_{out})/K_v]^{0.5} \quad (2)$$

A dimensionless venturi pressure-difference ratio can be defined for both choked and nonchoked flows:

$$dP_r = [P_{out} - P_{sat}(T_{in})]/[P_{in} - P_{sat}(T_{in})] \quad (3)$$

The maximum dP_r for choked flow occurs where $Mc = M_{nc}$. This critical dP_r can be expressed as $dP_{r,crit} = 1 - K_v$. Under either the choked or nonchoked condition, the actual CV's measured mass flow rate (M_{act}) can be expressed in dimensionless form as the mass flow ratio, $M_r = M_{act}/M_c$. The mass flow ratio for a nonchoked liquid flow can be expressed as

$$M_r = M_{act}/M_c = [(1 - dP_r)/K_v]0.5 \quad (4)$$

Overflow Problem Description

In the classic theory of the operation of CV, cavitation is normally assumed to occur whenever dP_r is less than the critical value, $dP_{r,crit}$. Nonchoked flow is limited to $dP_r > dP_{r,crit}$ ($M_r < 1$). However, this is not always the case in the GTA tests. Once dP_r exceeds $dP_{r,crit}$, the flow in the CV becomes all

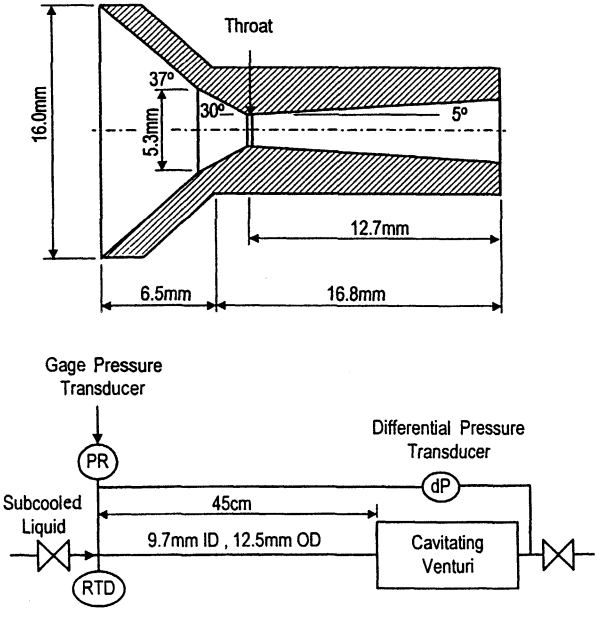

Fig. 1 Simplified schematic of CV's geometry and test section.

liquid. This type of flow tended to persist as dP_r decreased, even at values much lower than $dP_{r,crit}$. This phenomenon was dubbed overflow. During overflow, the pressure at the throat, P_{th}, was lower than $P_{sat}(T_{in})$. Thus, the liquid at the throat was superheated. The GTA test also confirmed that CV continued to persist as a nonchoked operation until dP_r was dropped to a value much lower than $dP_{r,crit}$. The point at which CV resumes its choked condition is called the rechoking point. Once cavitation is induced, CV is back to a normal choked operation.

Throat Superheat Required at Cavitation Inception

During all-liquid overflow the throat superheat [defined as $dP_{sup} = P_{sat}(T_{in}) - P_{th}$], using Bernoulli's equation and assuming zero friction loss, can be expressed as[2]

$$dP_{sup} = dP_{sub}[(1 - dP_r)/K_v - 1] \quad (5)$$

Experiment

The CV test loop is made of insulated copper tubes with 7.5 mm i.d. In this loop, pure water is stored in a 10-l stainless-steel tank that has an electric heater an refrigerating circulator for temperature control (293–363 K). A ball valve upstream of each CV is used to adjust the inlet pressure, and the CV outlet pressure and its pressure-difference ratio are varied through a needle valve located downstream of each CV. The instrumentation for the CV test section is also shown in Fig. 1. Two CVs with throat diameters of 0.91 and 1.16 mm are tested. The flow meter, which is mounted upstream of the CV test section, has a calibrated measurement range from 1.17×10^{-5} to 3.33×10^{-5} m^3/s, with an accuracy of $\pm 0.2\%$. Thermocouples have an accuracy of ± 0.5°C. The pressure transducers have a range from 0 to 1374 kPa, and an accuracy of $\pm 1\%$ of measured value. The differential pressure transducers had a range from 0 to 106 kPa, and an accuracy of $\pm 1\%$ of measured value. Data from the tests were collected through a data-acquisition system, with a sampling rate of one data point per second. Afterward, a spreadsheet (Microsoft Excel) was used to calculate various parameters, i.e., inlet subcooling, loss coefficient, mass flow ratio, pressure ratio, and the superheat at all of the test points.

Before starting the CV test, water in the container was held up to 355 K for 1 h for degassing. During each test process, the downstream needle valve was slowly cycled between the extreme positions. Variations of the P_r and M_r were analyzed to determine the loss coefficient and identify the choked, unchoked, overflow, and the rechoked operations. All CV mapping data were taken at set points with five water temperatures (298, 308, 330, 343, and 355 K), and three inlet pressures (239, 274, and 313 kPa). The inlet subcooling data was ranging from 180 to 310 kPa.

Test Results and Discussion

Two CVs with throat diameters of 0.91- and 1.16-mm CVs were tested in this study. A typical result at 343 K is shown in Fig. 2. Once the pressure ratio exceeded the critical value $(1 - K_v)$, the CV operation changed to nonchoked flow, and this nonchoked flow persisted even when the pressure ratio was decreased well below the critical value. The dashed line in Fig. 2 is the prediction of the CV overflow path based on Eq. (4). In the nonchoked flow regime for $dP_T > 1 - K_v$, the value of K_v is approximately equal to 0.19 for the 0.116 mm CV and 0.22 for the 0.91-mm CV. As shown in Fig. 2, the value of dP_r at the cavitation inception is slightly greater than the rechoked dP_r.

Because the pressure at the throat is not measured, the P_{th} value at the cavitation inception is estimated using Eq. (5), based on the measured values of dP_r, dP_{sub}, and K_v at the instant. Therefore, the average of the measured values of dP_r at cavitation inception and the rechoked dP_r was used in the calculation of the throat superheat at rechoking, $dP_{sup,rechoke}$. Concerning the $dP_{sup,rechoke}$ at the cavitation inception, Eq. (5) can be recast as the pressure ratio at the rechoking point as

$$dP_{r,rechoke} = 1 - K_v[(dP_{sup,rechoke}/dP_{sub}) + 1] \quad (6)$$

On the other hand, the onset of nucleation in pool boiling had been widely studied. Hsu[3] also used the pool boiling equation to determine the wall superheat requirement for the onset of nucleation in a pool boiling by assuming $r_c = r^*$, where r_c is the cavity mouth radius or the surface roughness, and r^* is the radius of spherical vapor. The superheat required for vapor nucleation can be shown as

$$dP_{sup} = 2\sigma/r_c \quad (7)$$

Figure 3 shows the $dP_{r,rechoke}$ data vs the inlet subcooling, the curved line of the $dP_{r,rechoke}$ prediction is based on Eq. (6) and the maximum superheat of 70 kPa for the 1.16-mm CV and 120 kPa for the 0.91-mm CV. The maximum superheat was used here to show the limit condition. It is adequate for the purpose of a conservative system design. The results of Fig. 3 indicate that the dP_r rechoking points scatter around the present predictions. The dP_r rechoking data for the GTA CV ammonia testing[2] it also compared with the prediction using Eq. (6), as shown in Fig. 3. Although large data scattering in

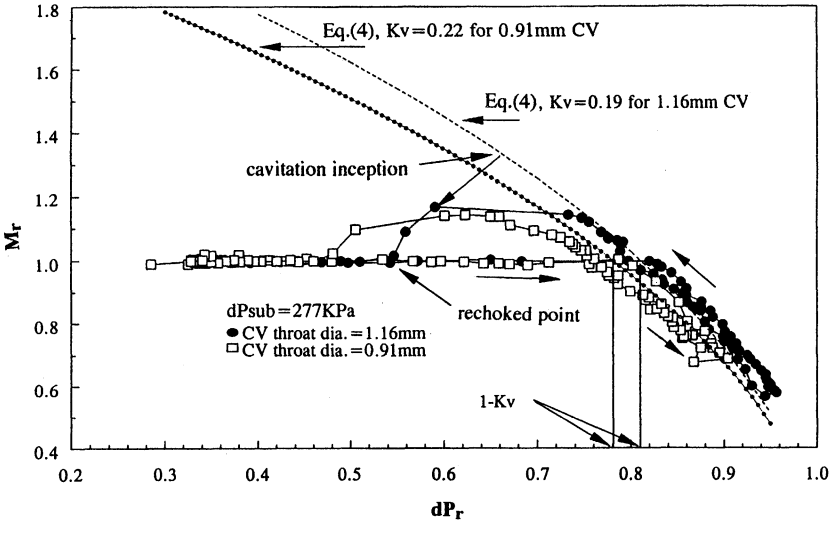

Fig. 2 CV overflow and cavitation recovery at 343 K.

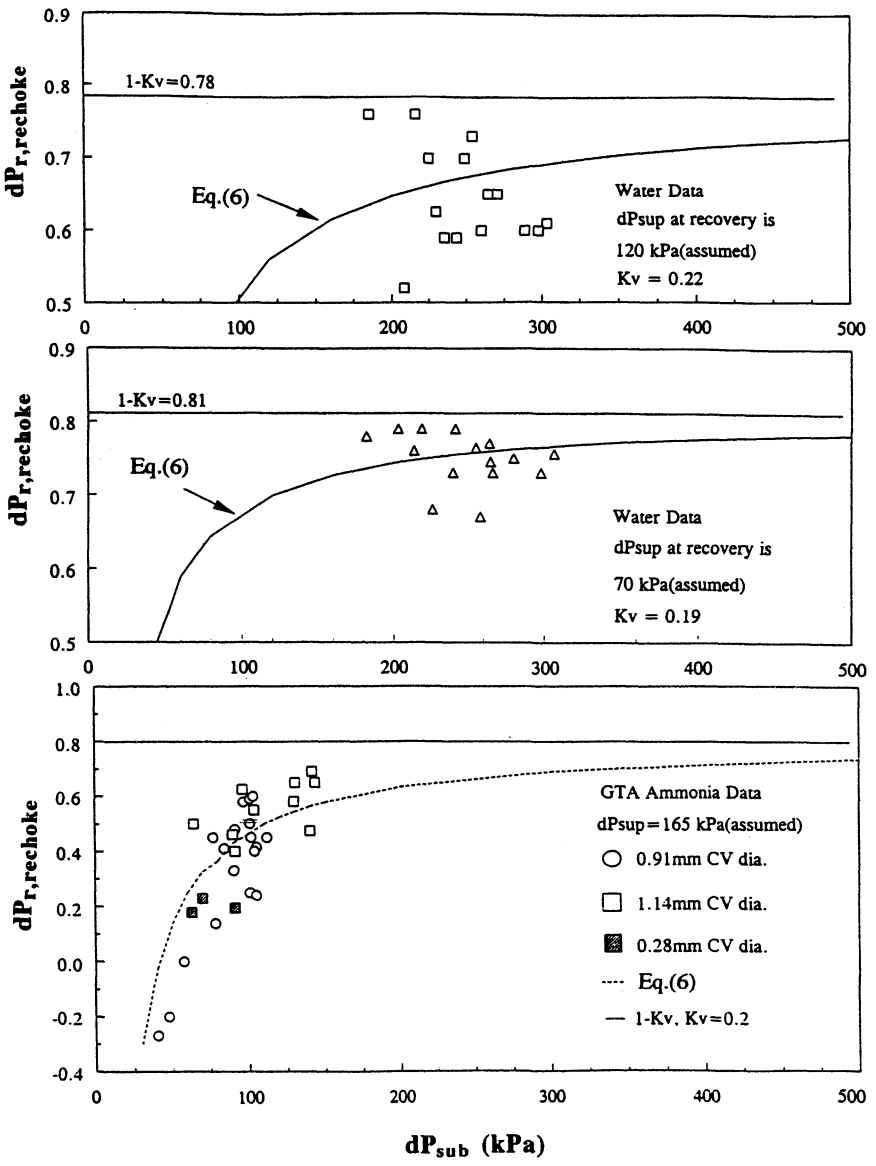

Fig. 3 Pressure-difference ratio at rechoking vs inlet subcooling.

Fig. 3 are a result of the large variation of the throat superheat at cavitation inception, the trend of dP_r at rechoking vs inlet subcooling is consistent with the prediction of $dP_{r,\text{rechoke}}$ using Eq. (6). Figure 3 also shows that the pressure ratio required for rechoking will approach to the critical pressure ratio ($dP_{r,\text{crit}} = 1 - K_v$) as the inlet subcooling increases to the order of 1000 kPa. This is the reason why the overflow problem was not reported in the typical industrial applications.

Apparently, Eq. (6) is very useful in determining dP_r required for rechoking. To use Eq. (6) for determining $dP_{r,\text{rechoke}}$ for a given inlet subcooling, the values of K_v and the throat superheat must be known. The loss coefficient is usually empirically obtained; however, no superheat correlation is available at the cavitation inception for CVs. The surface cavity sizes for a commercially finished drilling surface is typically in the ranges of 1.8–6.3 μm for an average application.[4] Assuming the cavity size for the two tested CVs in the preceding range, then superheat required at cavitation inception for the five inlet temperatures can be calculated using Eq. (7).

Using cavity sizes at 1, 2, and 5 μm, Eq. (7) was used to estimate the pool boiling superheat required for water in the tested temperature range of 298–355 K.[5] The predicted superheat curves were compared to the superheat data, the curves with cavity sizes of 2 and 5 μm are in the same order compared with the large scatter data that is because of the chaotic nature of the nucleation boiling phenomena. Based on this comparison, the tested CV surface cavity size may be approximately assumed as 2 μm. However, using the same CVs in the GTA ammonia testing, the maximum superheat obtained was 230 kPa, which implies the surface cavity size is 0.2 μm^2. This discrepancy between the water and ammonia data indicates that the CV throat superheat at cavitation inception is not dominated by the onset of nucleation in pool boiling. Should nucleation dominate, the superheat corresponding to ammonia and water is expected to differ by the ratio of 2.5:1 (because of the difference in surface tension). That means water would give a 650 kPa superheat if the surface cavity size of the tested CVs was indeed 0.2 μm. Because the Reynolds number was observed as an important factor for CV cavitation inception,[1] the factors that influence the onset of boiling in subcooled convection flow should be considered in future studies. Hopefully, with more test data in the future, a correlation concerning CV's behavior on throat superheat at rechoking can be established, which will be very useful for accurately predicting the choked flow recovery.

Conclusions

1) To completely avoid the dual mode operation, CV must always satisfy $dP_r < dP_{r,\text{crit}}$ in the overflow condition.

2) At a fixed inlet temperature and pressure the CV with the bigger throat diameter will have a higher rechoked pressure-difference ratio because of the lower loss coefficient.

3) If overflow is induced in CVs, Eq. (6) would permit an estimate of the pressure-difference ratio at cavitation inception.

4) According to the comparison of the test results and the analysis, the pressure-difference ratio at rechoking can be reasonably predicted using Eq. (6) at a given loss coefficient and inlet subcooling using the superheat that was found experimentally.

Acknowledgments

The authors wish to acknowledge the support provided by the National Science Committee, Taiwan, Republic of China, Research Grant NSC 86-2221-E-224-020, for making this study possible. They also acknowledge the invaluable assistance of E. K. Ungar at NASA Johnson Space Center.

References

[1]Hamitt, F. G., Ahmed, O. S. M., and Hwang, J.-B., "Performance of Cavitating Venturi Depending on Geometry and Flow Parameters," *Proceedings of the ASME Cavitation and Polyphase Flow Forum*, American Society of Mechanical Engineers, New York, 1976, pp. 18–21.

[2]Ungar, E. K., Dzenitis, J. M., and Sifuentes, R. T., "Cavitating Venturi Performance at Low Inlet Subcooling: Normal Operation, Overflow and Recovery from Overflow," *ASME Symposium on Cavitation and Gas-Liquid Flows in Fluid Machinery Devices*, FED-Vol. 190, American Society of Mechanical Engineers, New York, 1994, pp. 309–318.

[3]Hsu, Y. Y., "On the Size and Range of Active Nucleation Cavities on a Heating Surface," *Journal of Heat Transfer*, Vol. 84, No. 1, 1962, pp. 207–216.

[4]Avallone, E. A., and T. Baumeister, T., III, *Mark's Standard Handbook for Mechanical Engineers*, 9th ed., McGraw–Hill, New York, 1987.

[5]Liou, S. G., Chen, I. Y., and Sheu, J. S., "Testing and Evaluation of Small Cavitating Venturis with Water at Low Inlet Subcooling," *Proceedings of the Space Technology and Applications International Forum*, American Inst. of Physics, Woodbury, NY, 1998, pp. 479–487 (CP420).

Combined Conduction and Radiation Heat Transfer in a Cylindrical Medium

C. K. Krishnaprakas*
ISRO Satellite Centre, Bangalore 560 017, India

Nomenclature

$I_b(T)$ = blackbody radiation intensity, W/m^2-sr
$I(\tau, \hat{s})$ = radiation intensity at τ in the direction $\hat{s}$, W/m^2-sr
k = thermal conductivity of the medium, $k_0[1 + \alpha(T - T_1)]$, W/m-K
N_c = conduction–radiation number, $k_0\beta/4\sigma T_1^3$
$\hat{n}$ = normal vector to the surface
$p(\hat{s}, \hat{s}')$ = scattering phase function
$p(\mu_p)$ = single-scattering phase function
q = heat flux, W/m^2
r = radius of the cylinder, m
$\hat{s}$ = radiation direction vector
$\hat{s}_s$ = direction vector of the specularly reflected radiation from the boundary surface
T = temperature, K
α = coefficient for thermal conductivity variation, K^{-1}
β = extinction coefficient, $\kappa + \gamma$, m^{-1}
γ = scattering coefficient, m^{-1}
ε = emittance of boundary surface
η = direction cosine of $\hat{s}$ with the axis that is mutually orthogonal to the radius vector and the cylinder axis, $\sin\phi \sin\varphi$
θ = dimensionless temperature, T/T_1
κ = absorption coefficient, m^{-1}
μ = direction cosine of $\hat{s}$ with the radius vector, $\cos\phi \sin\varphi$
ν = variable thermal conductivity parameter, $k_0\alpha\beta/4\sigma T_1^2$
ρ = reflectance of the boundary surface, $\rho^d + \rho^s = 1 - \varepsilon$
ρ^d = diffuse reflectance of the boundary surface
ρ^s = specular reflectance of the boundary surface
σ = Stefan–Boltzmann constant, W/m^2-K^4
τ = optical depth of the medium at radius $r = \int_0^r \beta\, dr$
ϕ = angle between $\hat{s}$ and cylinder axis
ψ = azimuthal angle of $\hat{s}$ in the plane perpendicular to cylinder axis
Ω = solid angle, sr
ω = scattering albedo, γ/β

Subscript
1, 2 = boundary surfaces

Received Nov. 12, 1997; revision received March 11, 1998; accepted for publication May 4, 1998.

*Engineer, Thermal Systems Group.

Introduction

COMBINED conduction and radiation heat transfer in an absorbing, emitting, and scattering medium occurs in many engineering applications such as thermal insulation systems for cryogenic and space applications, propulsion systems, fluidized beds, optical engineering, solar engineering, nuclear engineering, atmospheric sciences, astrophysics, etc. Mathematical formulation of the problem leads to a complicated nonlinear integrodifferential system that is difficult to solve. In particular, coupled conduction and radiation heat transfer in planar systems has received the most attention by far, as reviewed by Viskanta[1] and Howell.[2] Relatively little work has been done for problems with cylindrical geometry despite their occurrence in many engineering applications. Fernandes and Francis[3] solved the coupled conduction and radiation problem for a gray absorbing, emitting, and isotropically scattering concentric cylindrical medium using a Galerkin finite element method. Pandey[4] solved the problem numerically using the undetermined parameters method, but did not consider scattering in the analysis. Harris[5] included anisotropic scattering in the analysis using the spherical harmonics method to solve the radiative transport equation.

The success of conduction/radiation analysis for cylindrical geometry depends to a large extent on the accurate modeling of the radiation field. Exact treatment of the radiative flux within a cylindrical medium is available for only very simple cases. To analyze a general problem, i.e., including anisotropic scattering, specular-diffuse boundaries, etc., alternate methods are to be resorted. Methods like Monte Carlo method or the Hottel's zone method, although accurate, require much computer time and storage and are not grid compatible with the other conservation equations. For higher-order approximations to the solution, the spherical harmonics method or the discrete ordinates method (also known as the S_N method) may be attempted.[6] Being differential in form, these methods are also grid compatible with the other conservation equations. Spherical harmonic methods involving complex mathematical manipulations and methods beyond P_3 makes the analysis too cumbersome. Compared to all of the other methods, the S_N